Effect of Autoclave Cure Time and Bonded Surface Roughness on the Static and Fatigue Performance of Polyurethane Film Adhesive Single Lap Joints

Isotta Morfini, Luca Goglio*, Giovanni Belingardi*, Sayed A. Nassar**

Fastening and Joining Research Institute (FAJRI)

Department of Mechanical Engineering

Oakland University, Rochester, Michigan 48309 USA

*Department of Mechanical and Aerospace Engineering, Politecnico di Torino, Turin, Italy

Abstract

This study investigates the effect of autoclave cure time and bonded surface roughness on the static and fatigue performance of film-adhesive single lap joints. Joint static performance is assessed in terms of its load transfer capacity in a quasi-static tensile-shear test to failure. Effect on fatigue life under a mean and cyclic tensile-shear amplitude is also investigated. Two levels autoclave cure (soak) time and two levels of bond surface roughness are investigated. All other autoclaving process variables are kept constant; namely, the ramp rate of temperature rise/cooling, pressurization/depressurization, as well as the cure temperature and cure pressure levels. Test joints are made of aluminium-aluminium or aluminium-magnesium adherends, joined with a polyurethane film adhesive. The results suggest that: an increase of the surface roughness is beneficial to static strength and detrimental to fatigue strength; an increase of the autoclave soak (cure) time is beneficial both to static and fatigue strength. Test data, failure mode analysis, discussion, observations and conclusions are provided.

Keywords: A. polyurethane; B. aluminium and alloys; C. lap-shear, fatigue;

autoclave bonding, film adhesive

** Fellow ASME- Corresponding Author e-mail address: nassar@oakland.edu

1. Introduction

Adhesive bonding is increasingly becoming a viable option for load bearing joints made of similar and/or dissimilar materials in many lightweight mechanical, structural, automotive, aerospace, biomedical, and microelectronics systems [1]. Increased demand for lightweight and multi-material use for design optimization, high performance, energy and fuel economy, and emission concerns are all contributing to the increased demand for adhesive bonding [2]. Reliability of adhesively-bonded joint under external applied service loads is paramount in safety-related and/or critical systems. Surface treatments play a key role regarding this aspect, both for the strength of the adhesion obtained and in terms of durability, especially under atmospheric degradation. Special pre-treatments (i.e. prior to bonding) have been developed for light alloys, typically based on electrochemical treatments such as chromic acid (CAA) or phosphoric acid (PAA) anodising [3]. Obviously, usage of chemicals poses additional problems regarding their disposal. A wide survey on the surface pretreatments suitable to improve adhesion for aluminium alloys was presented by Critchlow and Brewis in [4]. In addition to the chemical treatments of the surface, also the roughness influences durability; Critchlow and Brewis in [5] studied this effect on epoxy-aluminium joints, distinguishing between microroughness left by chemical treatments and macroroughness (feature size > 1 μm) produced by grit-blasting. On a different scale (tens of μm), and in the case of steel-composite joints, the effects of the roughness causing interlocking which improves adhesion strength was investigated by Kim et al. [6]. Goglio and Rezaei [7] compared the effects on durability of different pretreatments for aluminium joints, ranging from simple degreasing-roughening to the use of a conditioner or PAA; a contamination technique to accelerate durability tests was also tried.

The above-mentioned durability studies concern static strength; however, for industrial applications a major issue is the strength under fatigue loading. A milestone study was presented by Crocombe

and Richardson [8] that considered, for steel adherends and epoxy adhesive, several joint configurations and the influence of the mean load on fatigue life.

Several studies investigated the effect on fatigue life of bonded joints exerted by surface treatment and roughness, as well as by environmental factors such as moisture. In this survey the attention is focussed on aluminium joints and recent results. Rushfort et al. [9] tested aluminium single-lap specimens bonded with an epoxy, comparing the effect of the exposure to moisture and a silicon-based pretreatment; untreated joints exposed to moisture exhibited remarkably lower fatigue strength. Similarly, Abel et al. [10] investigated the effect of a silane primer on the fatigue strength of tapered double-cantilever beam joints made of aluminium bonded by an epoxy tape; results in terms of fracture energy, obtained under "dry" and "wet" conditions were compared, showing the importance of the pretreatment. An epoxy tape (Cytec FM73) was also used to investigate the effect on fatigue life of a silane pretreatment by Underhill and DuQuesnay in [11] and of cladding the adherends by Nolting et al. [12]. The same tape was used by Shenoy et al [13] to assess the residual strength after fatigue degradation and propose a prediction model. A model for the prediction of the fatigue failure based on fracture mechanics was used by Pirondi and Moroni [14] for lap joints made of aluminium adherends and three different types of adhesives (namely one acrylic and two epoxies). Jen and Ko [15] investigated the effect of single lap joint dimensions (overlap length, adhesive thickness) on the strength of aluminium adherends bonded with an epoxy, finding that the interfacial peeling stress has the major effect on debonding.

Hurme and Marquis [16] investigated hybrid joints that combine adhesives and bolts. They examined fatigue damage in the bonded interfaces through scanning electron microscopy and concluded that a progressive damage in the adhesive and fretting fatigue are the major responsible for fatigue failure. Test specimens from high-strength steel sheets were grit blasted and the interfaces were bonded with a two-component structural epoxy adhesive. Scanning Electron Microscope (SEM) analysis revealed that the fatigue failure was caused by multiple cracks, voids

and inclusions. That resulted in localized stress concentration at some peaks and valleys of the surface topography and existing void inclusions. Stress concentration (not poor adhesion) was the main reason for crack formation and propagation at the interface.

All the above-mentioned studies considered adhesives of epoxy or (more rarely) acrylic type; none of them used polyurethane adhesives in film form. Film adhesives of this type offer several advantages in terms of ease of storage and application, they require temperature and pressure to be activated, which are typically applied with an autoclave process. Regarding this point, no previous work seems to have taken into account on a systematic basis the effect of autoclave cure time and pressure, as well as surface preparation of the bond area, on the static strength (i.e. load transfer capacity - LTC) and fatigue strength of the adhesion between light alloy adherends and polyurethane film,

Due to the lack of studies that provide in-depth quantitative analysis of the effect of single and multiple-variable interaction of key process factors on the reliability of autoclave-bonded joints and/or panels, this investigation provides a baseline study of some of those variables. In general, the main autoclave process variables include the levels of cure temperature and pressure, the duration of cure (soak) time at peak temperature and pressure, the autoclave rate of temperature rise and cooling, as well as the initial autoclave pressurization rate and final depressurization rate during the curing process.

This baseline study focuses on the effect of some of the above-mentioned process variables on the static and fatigue performance of autoclave-bonded film adhesive single lap joints (SLJ); namely, the effect of cure (soak) time for two levels controlled surface roughness, and two combination of adherend materials. The objective of this investigation is to understand which are the most influential on the considered results. However, our intention was not to build a behavioural model from the experimental data but just to make clear if the selected factors have influence and to what extent.

2. Material Selection and Autoclave Bonding Process

Test single lap joint adherends were made of aluminium alloy 6061-T6511 and magnesium alloy AZ31B-H24 bonded with PE399, a commercial high-performance aliphatic polyether film adhesive produced by Huntsman. Tables 1-2 summarize the mechanical properties of joint and film adhesive materials used in this study.

Table 1. Mechanical properties of the Al [17] and Mg [18] alloys.

Material	Density	Elongation	UTS	Young's Modulus E
	[g/cm^3]	(%)	[MPa]	[GPa]
Al alloy (6061-T6511)	2.7	9-13	260-310	70-80
Mg alloy (AZ31B-H24)	1.77	15	290	45

Table 2. Mechanical Properties of PE 399 Adhesive [19].

Property	Unit	Value
Tensile Strength	MPa	45
Elongation at break	%	500
100% Modulus	MPa	2

In autoclave film adhesive bonding technology, the adhesive sheet is placed on the bond area between the two metal adherends of the joint, which are then placed in a vacuum bag and subsequently positioned inside the autoclave to cure, according to the programmed set of bonding variable profiles for cure temperature and pressure as well as cure time.

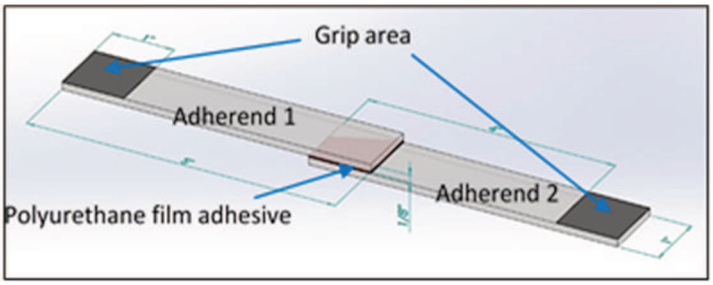

Figure 1. Configuration of Test Joints.

Figure 1 shows the SLJ standard geometry adopted for the joint mechanical characterization. Adherends coupon dimensions are 25.4 mm x 127 mm x 3 mm; thickness of the film adhesive is 0.6 mm on a square 25.4 mm x 25.4 mm bond area as illustrated in Fig.1. Two levels of surface roughness of bonded region were generated by manual sanding using fine (P2000 grit) or coarse (P150 grit) sand-paper until the roughness measurements became reasonably repeatable at various locations on the sanded surface. Sanding surfaces with fine or coarse sand paper would, respectively, create lower surface roughness designated as R1, or higher surface roughness designated as R2. Surface roughness was measured using a commercially available Wyko NT1100 optical profiler. Figure 2 shows the average surface roughness data (and +,– one standard deviation scatter bars) from each of the three test joints; roughness measurements were taken at different locations on the adherend bond area prior to bonding.

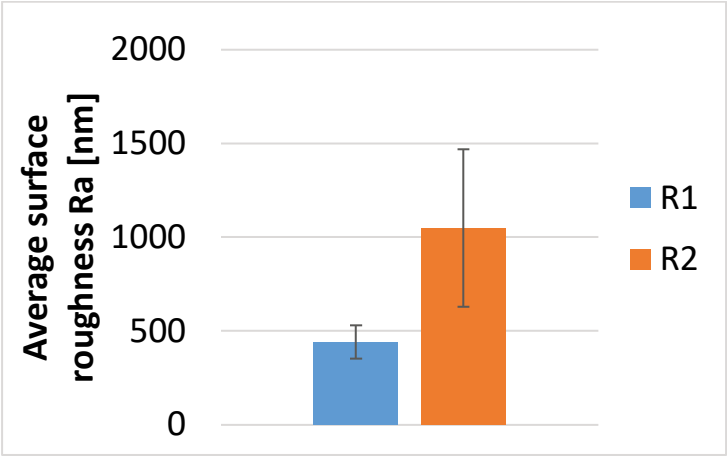

Figure 2. Average Roughness; bars show ± one standard deviation.

Prior to autoclave bonding process, all coupon surfaces were cleaned with acetone.

As previously defined, among the process variables that have been identified, for this introductory study, only the cure time duration during autoclave bonding was investigated, while keeping all other process variables unchanged. In particular, both the ramp rate of pressure and temperature, and the levels of cure temperature and cure pressure were maintained the same (fixed) the bonding autoclave bonding of all test SLJs in this study.

Tables 3 and 4 show detailed description of fixed setup values for the autoclave. Figures 3 and 4 show the two studied cure (soak) time durations namely 40 and 80 minutes (2400 s and 4800 s), which are respectively designated as t1 and t2 cure time levels.

Table 3. Level of fixed autoclave process parameters.

Heating / Cooling Rate [Fixed]	± 0.121 °C/s	(0.218 °F/s)
Cure Temperature [Fixed]	127 °C	(260 °F)
Pressurization Rate [Fixed]	± 0.719 Pa/s	(0.104 psi/s)
Cure Pressure [Fixed]	0.86 MPa	(125 psi)

Table 4. Cure (soak) time levels.

Cure (soak) time [s]	2400	4800
Cure time level designation	t1	t2

Both levels fall within adhesive supplier-recommended range.

Figures 3-4, respectively, illustrate the autoclave temperature and pressure profiles for the 40-minute (2400 s) and 80-minute (4800 s) durations of cure (soak) times.

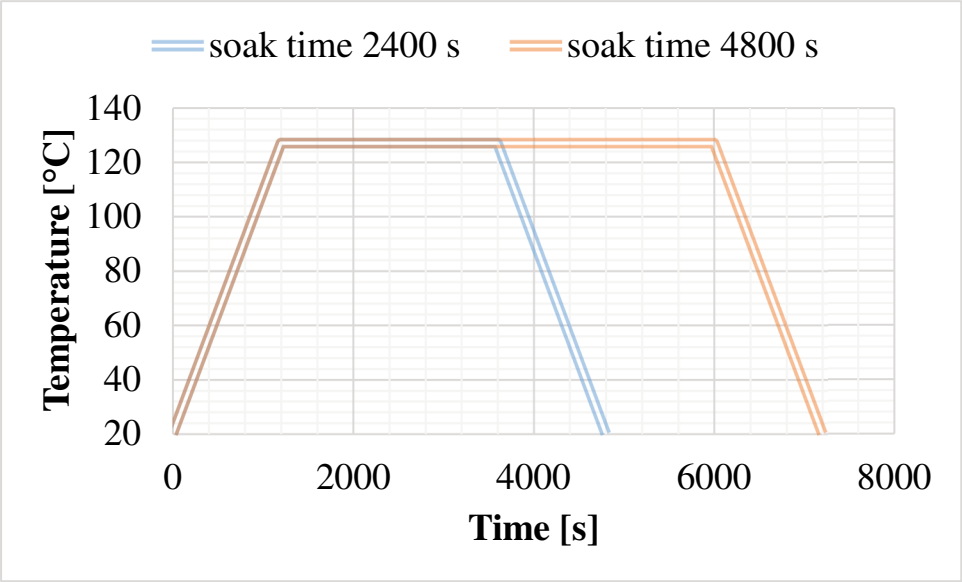

Figure 3. Temperature profile during autoclave bonding.

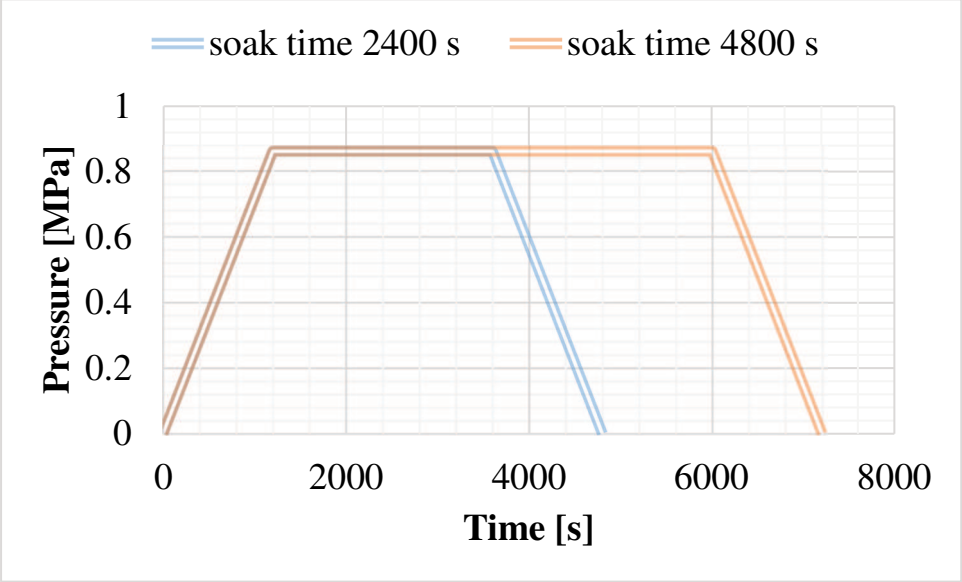

Figure 4. Pressure profile during autoclave bonding.

3. Experimental Procedure and Test Setup

This section outlines the respective procedures for static and fatigue testing of single lap joints under tensile-shear loading.

3.1. Static Testing

Upon the completion of autoclave bonding of single lap joints using respective process profiles, quasi-static tensile-shear testing of single lap joints were carried out using an MTS testing system that collects load-deformation data until fracture. The maximum load represents the LTC of test joints. Sample size of 3 replicas was used for each test. Tests were performed in accordance with the ASTM D1002 standard. Test load was applied at a constant speed of 1.27 mm/min. Dummy tabs of the same thickness as the adherends were used for gripping into the MTS jaws in order to minimize the bending effect. Figure 5 shows the static LTC data for two groups of test samples; namely, the four [same material] aluminium-aluminium joints on the left, and the other four [dissimilar materials] aluminium-magnesium joints on the right. In each group, respective LTC data is shown for two-variable/2-level combinations; namely, surface roughness levels R1 and R2, and cure time durations designated as t1 and t2.

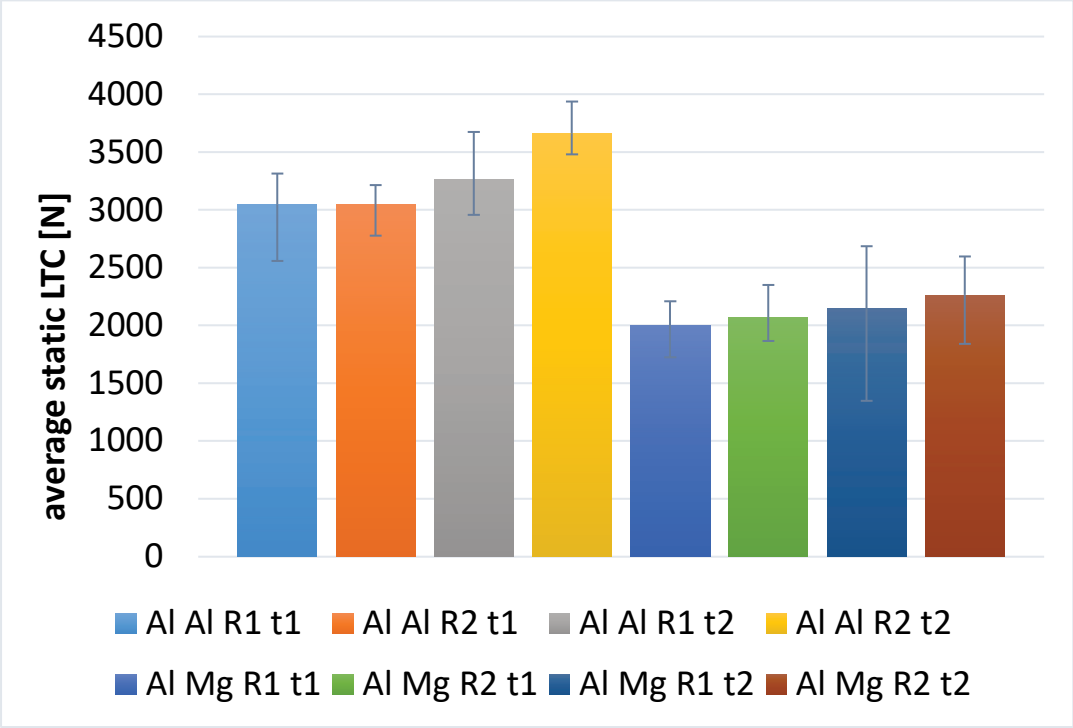

Figure 5. Static Load Transfer Capacity (LTC); bars show ± one standard deviation.

3.2. Fatigue Testing

Fatigue testing was devoted to explore the effect of the same two factors; namely, surface roughness and autoclave cure time, on the fatigue life. Tensile-shear fatigue tests were carried out at a frequency of 20 Hz using an MTS fatigue testing system. The mean load was kept constant at 50% of the respective average value of the static LTC. Two levels of cyclic load amplitude were used; namely, 2% and 20% of the respective average value of joint LTC.

Table 5 collects all the parameters used for the 8 different fatigue tests of the SLJ specimens in the case of the low amplitude (2% of the respective LTC). For each of the considered 8 different types of testing conditions, 3 replicas were done in order to obtain some (even if little) information about the typical scatter of the fatigue results; 24 tests were performed in total. Table 6 collects the values of the parameters used for the 8 different fatigue tests of the SLJ specimens in the case of high amplitude (20% of the LTC); however, in this case for each material pair (Al-Al or Al-Mg) unique values of mean load and amplitude were used, both based on the average LTC calculated between all four statics tests carried out for that pair. In each row of the table, the considered reference average value of LTC and the consequent mean load and amplitude values are reported. Also in these tests 3 replicas were done for each condition.

Table 5. Fatigue test parameters for low amplitude (2% of respective LTC).

SLJ parameters and static LTC data				Fatigue test loads at low amplitude	
Adherend materials	Roughness [µm] (Fig. 2)	Cure Time [min] (Figs 3-4)	Static LTC [N] (Fig. 5)	Mean load F_{mean} [N] (50% of LTC)	Amplitude F_{alt} [N] (2% of LTC)
Al-Al	R1(low)	40 (t1)	3045	1522	61
Al-Al	R2 (high)	40 (t1)	3042	1521	61
Al-Al	R1(low)	80 (t2)	3267	1633	65
Al-Al	R2 (high)	80 (t2)	3661	1831	73
Al-Mg	R1(low)	40 (t1)	2000	1000	40
Al-Mg	R2 (high)	40 (t1)	2066	1033	41
Al-Mg	R1(low)	80 (t2)	2148	1074	43
Al-Mg	R2(high)	80 (t2)	2263	1131	45

Table 6. Fatigue Test Parameters for High Amplitude (20% of overall average LTC).

SLJ parameters and static LTC data				Fatigue test loads at high amplitude	
Material	Cure Time [min]	Roughness [µm]	Static LTC [N]	Mean load F_{mean} [N] (50% of LTC)	Amplitude F_{alt} [N] (50% of LTC)
Al-Al	40 and 80	R1 and R2	3254	1627	651
Al-Mg	40 and 80	R1 and R2	2119	1060	424

4. Results and discussion

In this section, test data are presented and discussed for what concerns the effect of adhesive cure time and bond surface roughness on the static and fatigue performance of autoclave-bonded joints with film adhesive. Statistical Design of Experiment (DOE) data analysis using Minitab commercially available software [20] is provided for three variables at two levels each; namely, the

cure time designated as t1 and t2 levels, bonded surface roughness designated as R1 and R2 levels, and two joint material combinations (Al-Al and Al-Mg). Statistical data analysis performed on the basis of a full factorial plane discusses the relative significance of single and two-variable combinations to the static and fatigue life. This analysis is not finalised to derive a mathematical model but, as discussed in the introduction, the aim is to understand if each factor and interaction is influential on the result and to estimate the relative influence. This can be carried out on the basis of a two points analysis, while, obviously, in order to build a mathematical model a larger number of levels for each considered factor would be necessary in order to capture possible non-linearities.

4.1. **Variable Effect on the Static Strength (LTC)**

Firstly, by examining Fig. 5, the importance of the material pair is apparent. Al-Al joints exhibit larger strength, as the LTC is in the range 3000-3500 (and more) N, whilst the LTC of the Al-Mg joints is in general slightly above 2000 N. This dependence on material pair exceeds the statistical scatter of the results (see ± one standard deviation bars). Secondly, for a given material pair a slight effect of both roughness and soak (cure) time on the mean LTC values can be perceived, although within the statistical scatter.

A better insight is given by the Pareto Chart that shows the rank among the influencing factors that are listed from the most influencing (or significant) to the less influencing, as reported in Figure 6. It appears that the most important among the three studied factors is the adherend material pair, the other factors as well as the interactions are relatively less significant.

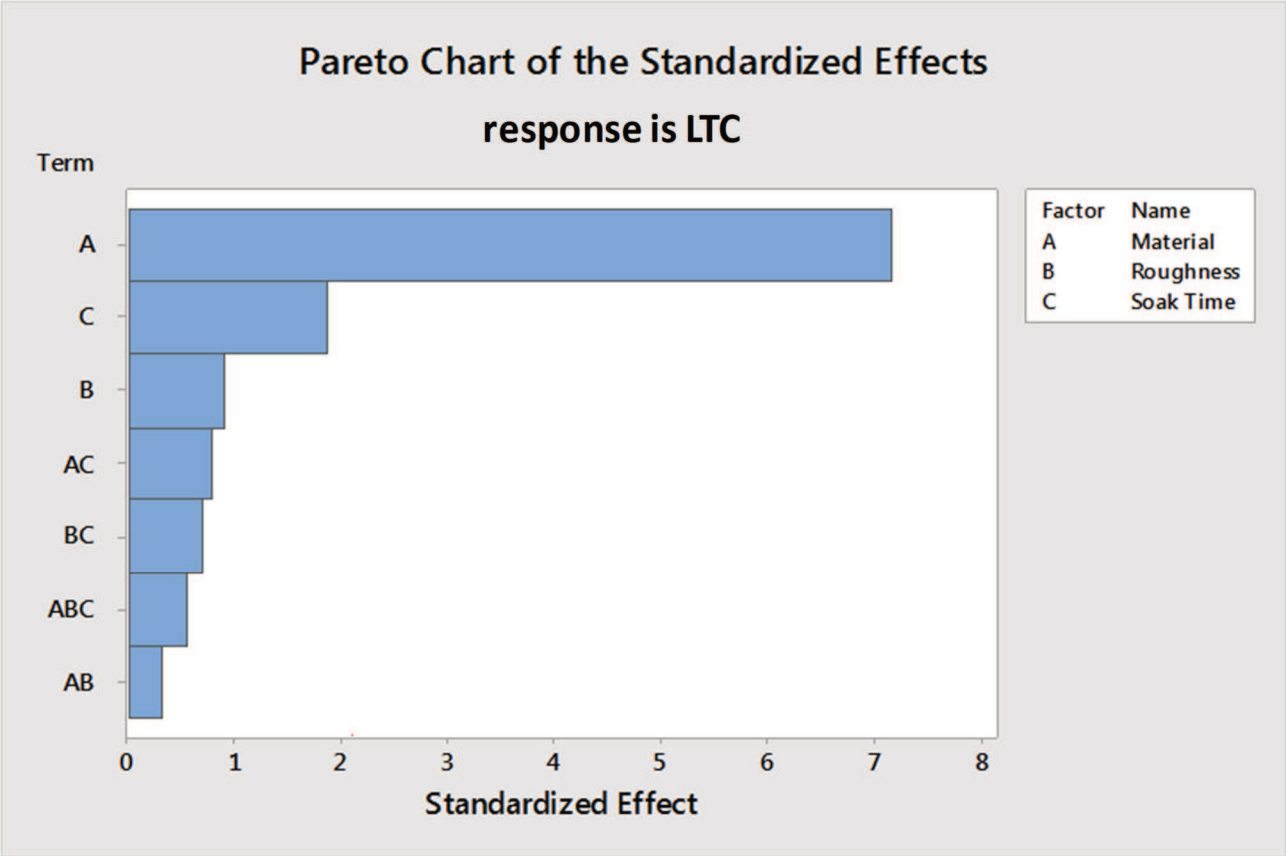

Figure 6. Pareto Chart for LTC of SLJ.

The role of the individual factors can be analysed by means of the plots in Figures 7-8, respectively for Al-Al and Al-Mg joints, which show that both surface roughness and cure time affect the static LTC of the tested joints. The straight lines in the diagrams are just evidencing trends and have not to be interpreted as a linear interpolation model. Higher surface roughness leads to an increase of the static strength LTC, and so does a longer cure time. A higher surface roughness creates a stronger mechanical interlocking bond between the adherends and the adhesive. The bond strength at the interface between the adherend and the adhesive is enhanced by the penetration of the polymer into the cavities and the pores of the substrate. Additionally, the rougher the surface is, the higher the energy dissipation required for causing static failure. Similarly, a longer curing time further improves the adhesion of the film to the metallic adherends and accordingly increases the static strength (LTC) of the tested joints.

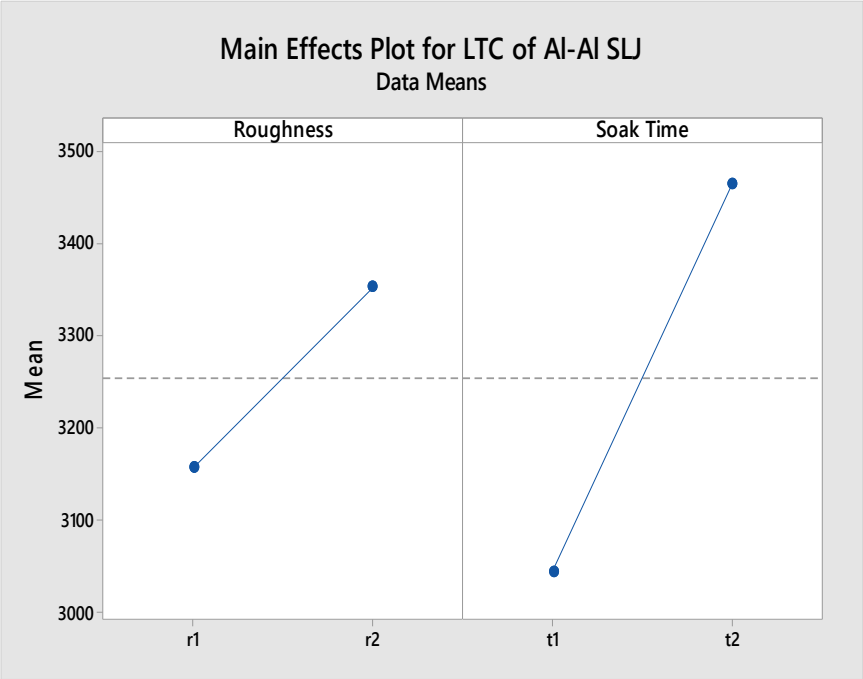

Figure 7. Main Effects Plot for LTC for Al-Al joints.

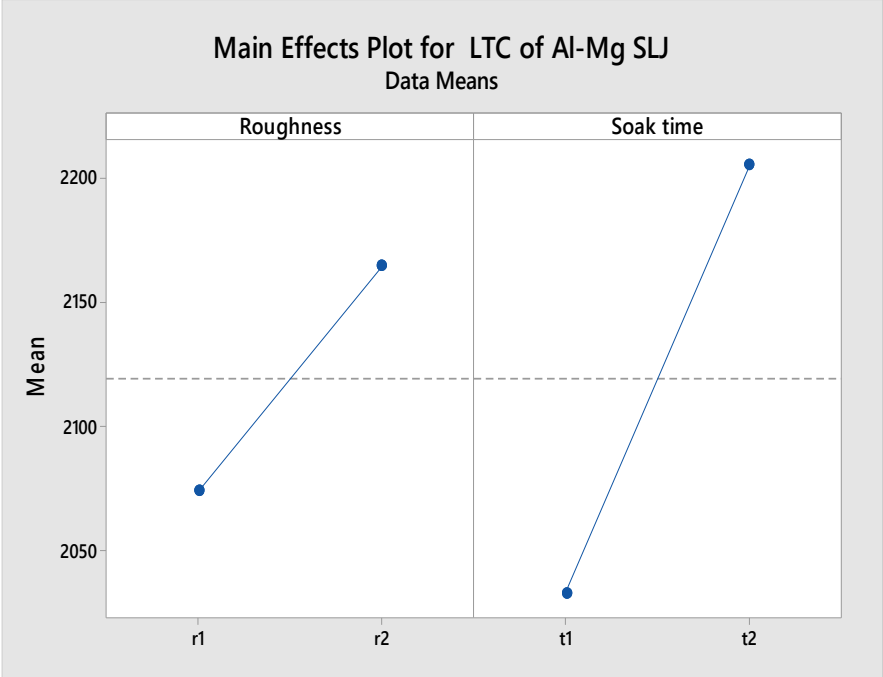

Figure 8. Main Effects Plot for LTC of Al-Mg joints.

3.2 Variable Effect on Joint Fatigue Life

For both Al-Al and Al-Mg joints, Figures 9 and 10, respectively, show the fatigue life in terms of cycles until joint failure under a cyclic alternating load (F_{alt}) and a mean load (F_{mean}) that are, respectively, equal to 2% and 50% of the static LTC relevant to each individual test joint configuration at 2 levels of surface roughness and 2 levels of cure (soak) time.

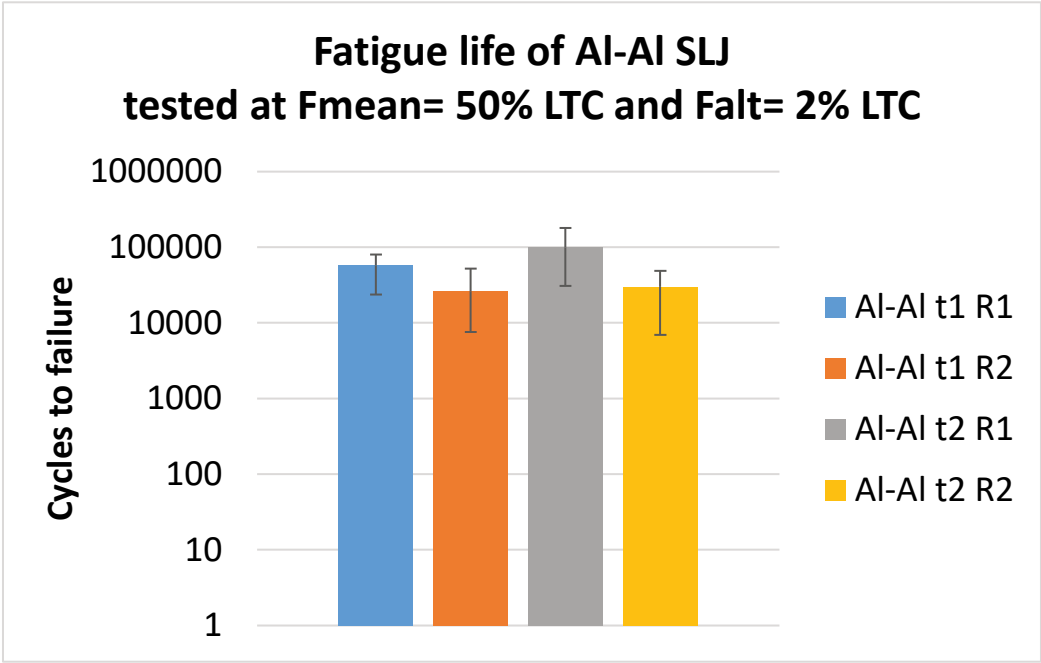

Figure 9. Fatigue Life data for Al-Al joints under F_{alt} = 2% of LTC.

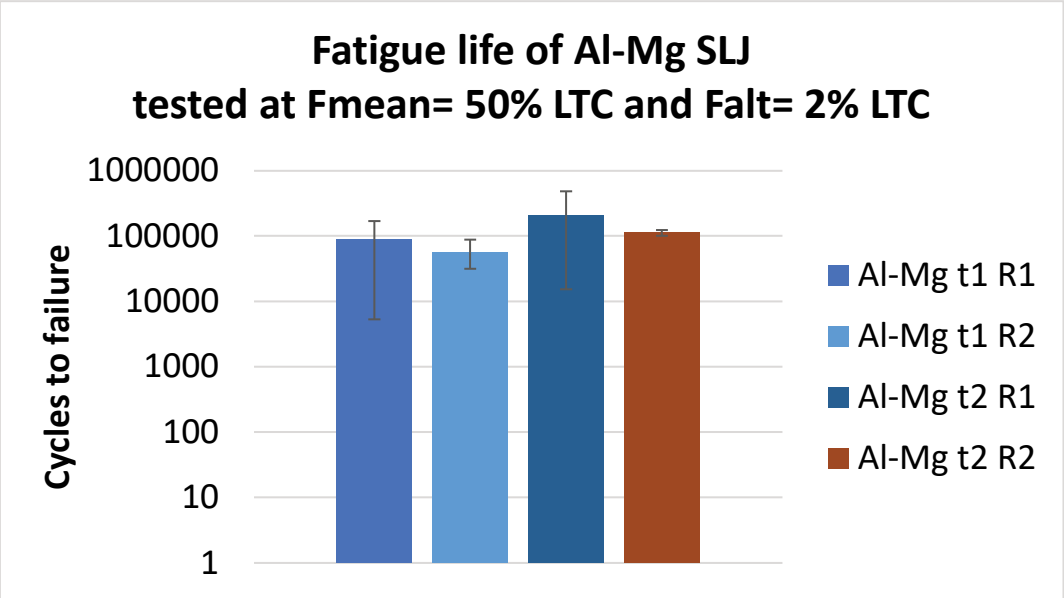

Figure 10. Fatigue Life data for Al-Mg joints under F_{alt} = 2% of LTC.

Similarly, Figures 11-12 show the test data on fatigue life under a higher cyclic alternating load equal to 20% of the respective overall average of static LTC for all Al-Al joints and that of all Al-Mg joints; the mean load is kept equal to 50% of the respective overall average joint static LTC.

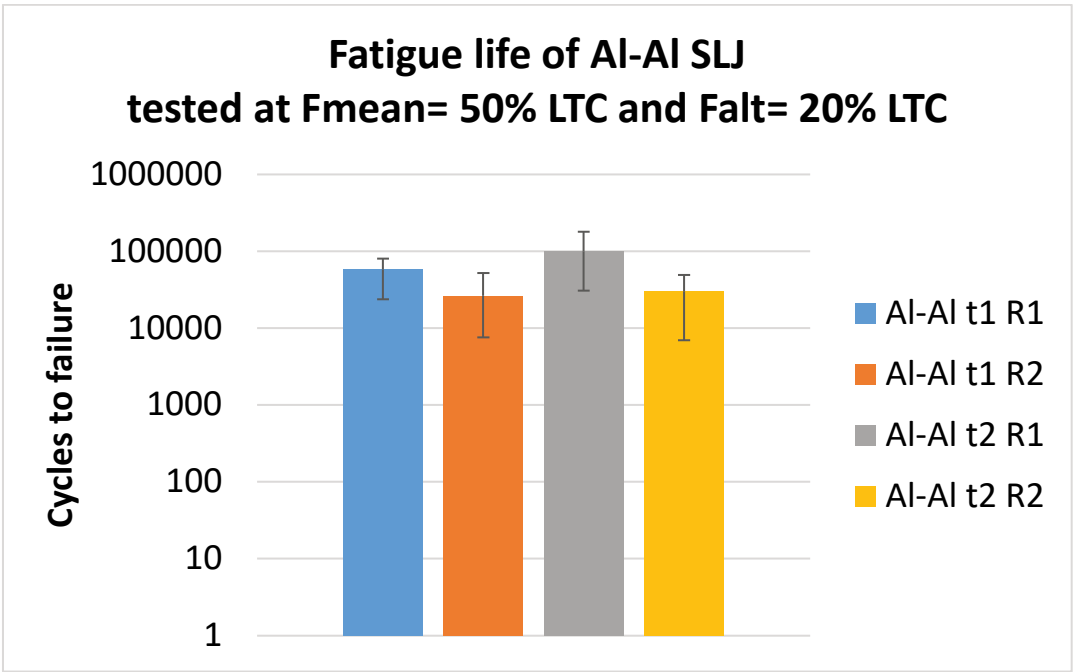

Figure 11. Fatigue Life for Al-Al Joints
(F_{alt} = 20% and F_{mean} =50% of overall average of all Al-Mg joints LTC).

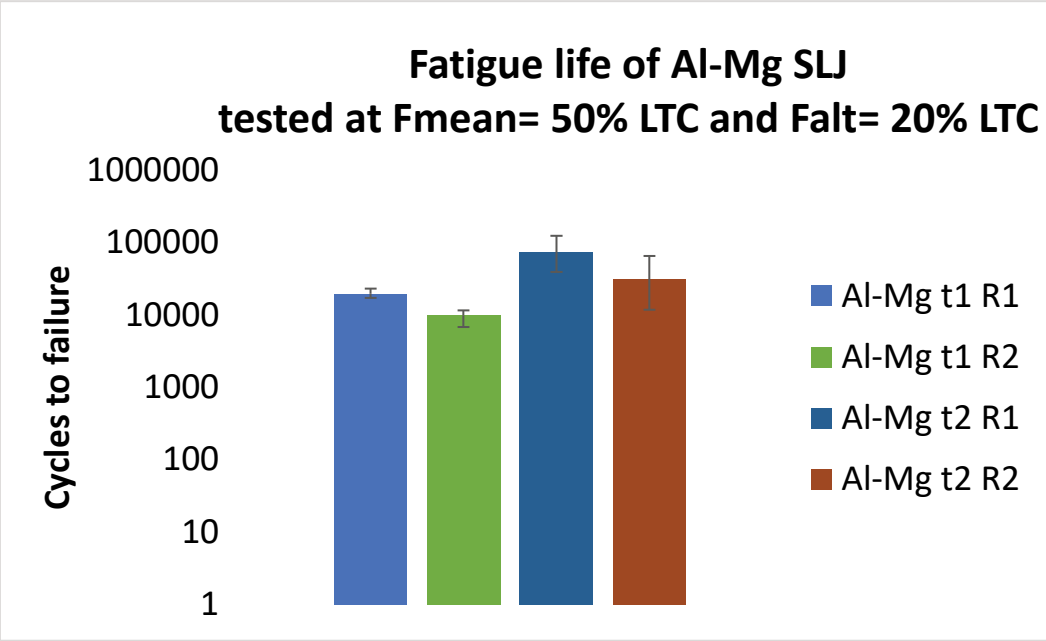

Figure 12. Fatigue Life for Al-Mg Joints
(F_{alt} = 20% and F_{mean} =50% of overall average of all Al-Mg joints LTC).

Contrary to its effect on increasing joint static strength (LTC) as reflected by the positive slope of the main effect (roughness) in Figs. 7-8, increasing the surface roughness does reduce the fatigue life, as reflected by the fatigue life data in Figs. 9-12, as well as by the negative slopes of the corresponding main effect charts in Figs. 13-16, for both Al-Al and Al-Mg joints, respectively, under both low and high alternating load amplitudes. A possible explanation for the reduction in joint fatigue life by increasing the roughness of bond surface is that, contrary to the case of static strength, the higher asperities of the rougher bond surface are more likely to act as crack initiators under cyclic fatigue loading. That would eventually lead to faster fatigue failure of the adhesion at the interface. Finally, it has been observed that dissimilar-material joints (Al-Mg) exhibited longer fatigue life than same material joints (Al-Al) under similar cyclic and mean loads (as percentage of their own static strength LTC). Such aspect is further commented in Section 4.3 in light of SEM inspection of fracture surfaces.

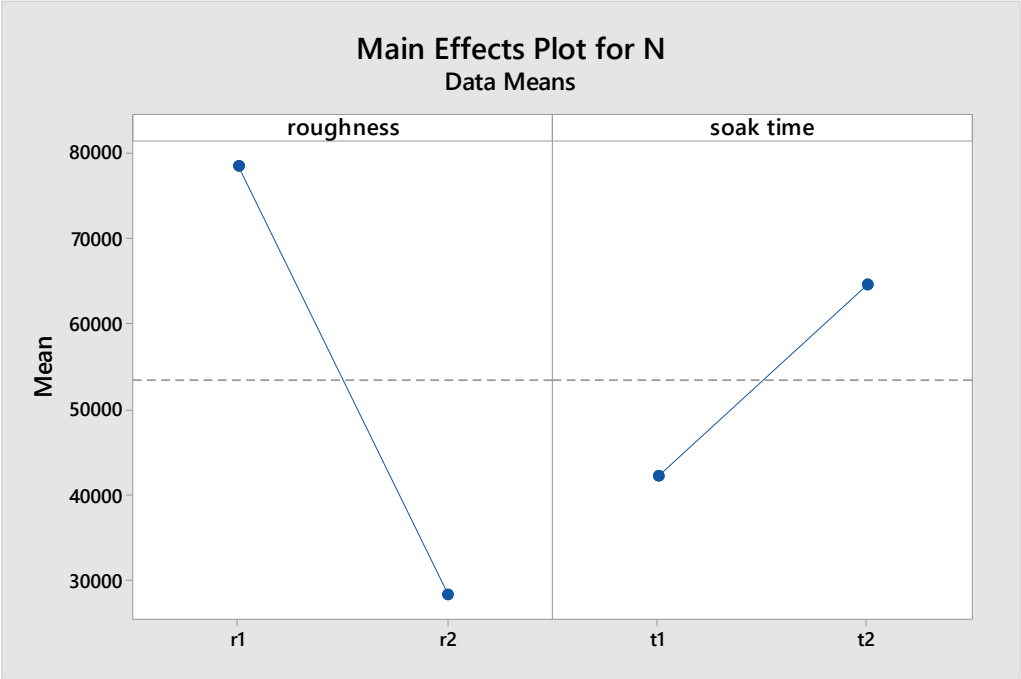

Figure 13. Main Effects Plot for Fatigue Life of Al-Al Joints under F_{alt}= 2% LTC.

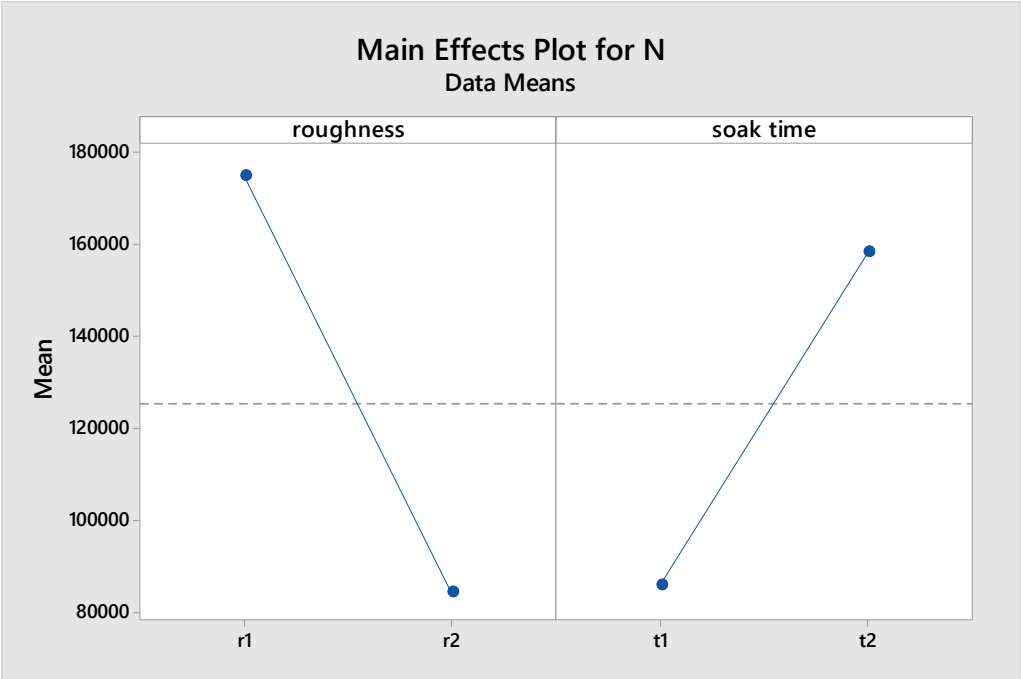

Figure 14. Main Effects Plot for Fatigue Life of Al-Mg Joints under F_{alt}= 2% of LTC.

As for the effect of cure time on joint fatigue life, Figures 9-16 show a similar trend to of the static testing; namely, the longer cure time (80 minutes) during the autoclave bonding process would increase the joint fatigue life as compared to the shorter cure time (40 minutes). Such increase in

fatigue life is mainly attributed to further curing of the adhesive, which generates a stronger adhesion between the polymeric film adhesive and metallic substrates.

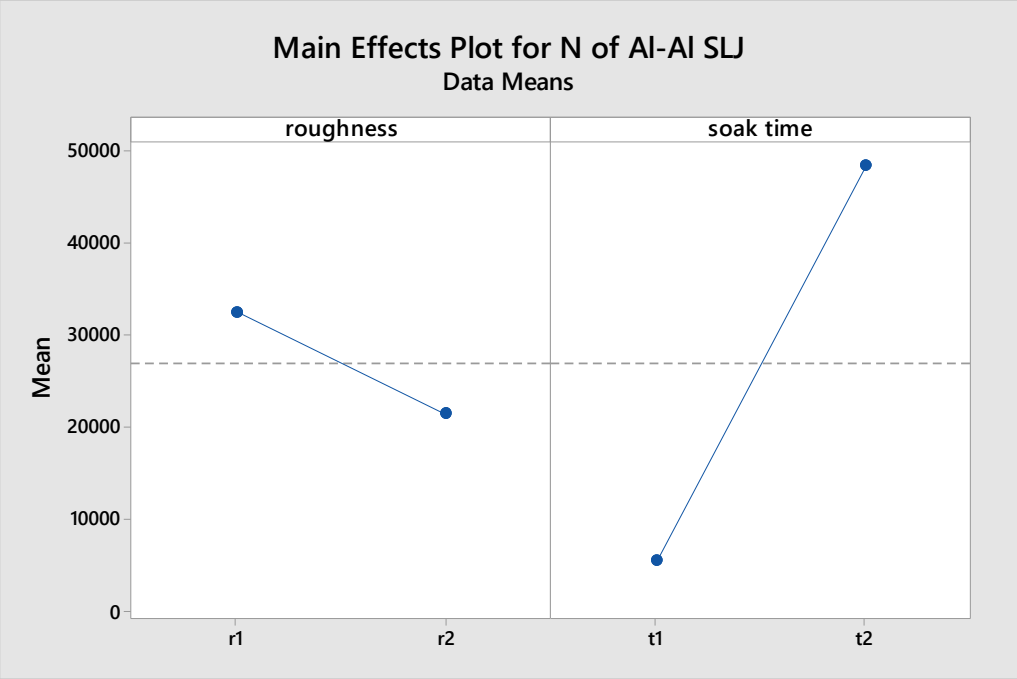

Figure 15. Main Effects Plot for Fatigue Life of Al-Al Joints under F_{alt}= 20% of LTC.

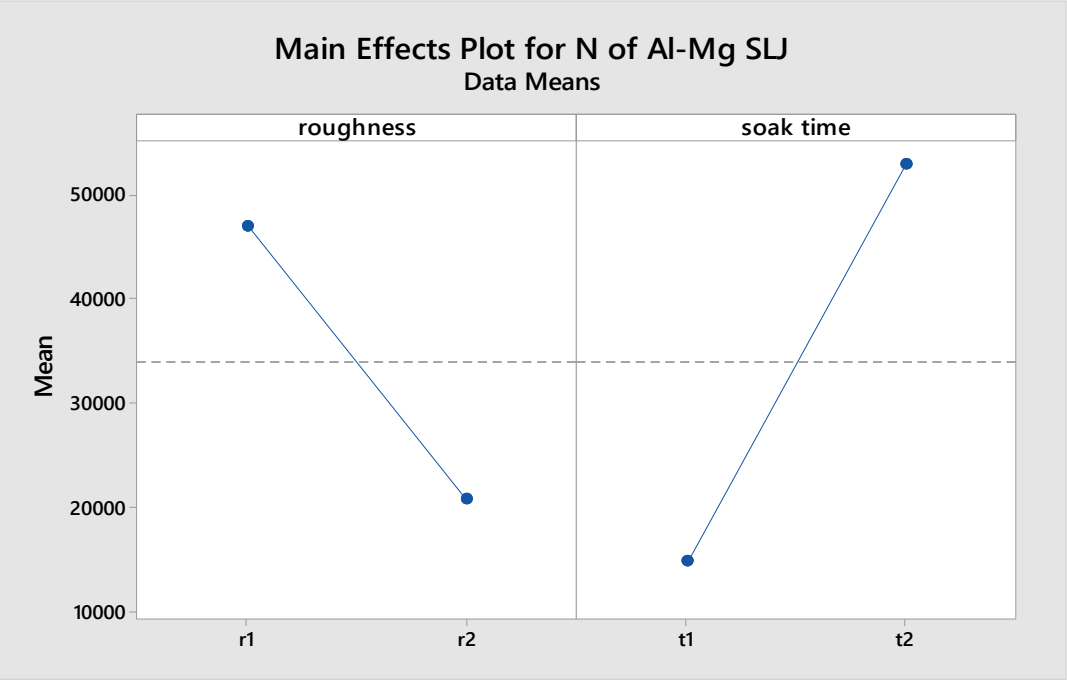

Figure 16. Main Effects Plot for Fatigue Life of Al-Mg Joints under F_{alt}= 20% of LTC.

Statistical analysis of the results by means of Pareto Chart shows quite different sorting list of the factors that are influencing the fatigue life with respect to what has been shown in figure 6 for the LTC. In particular, it can be noted that cure time has the most relative significance in terms of its effect on joint fatigue life (Fig. 17), followed by the surface roughness and the interaction between cure time and surface roughness. The pair of adherend materials, that was the most influencing factor for the LTC data analysis, is at the fifth position with rather low significance; this is simply due to the fact that the joints were fatigue tested under mean and alternating load levels proportional to their respective static strength LTC of the relevant material pair. Thus, the dependence on the material is nearly eliminated. It is worth noting that the effect of the interaction between two factors BC (roughness and soak time, respectively), and AB (material and roughness) still have some relative significance, although limited.

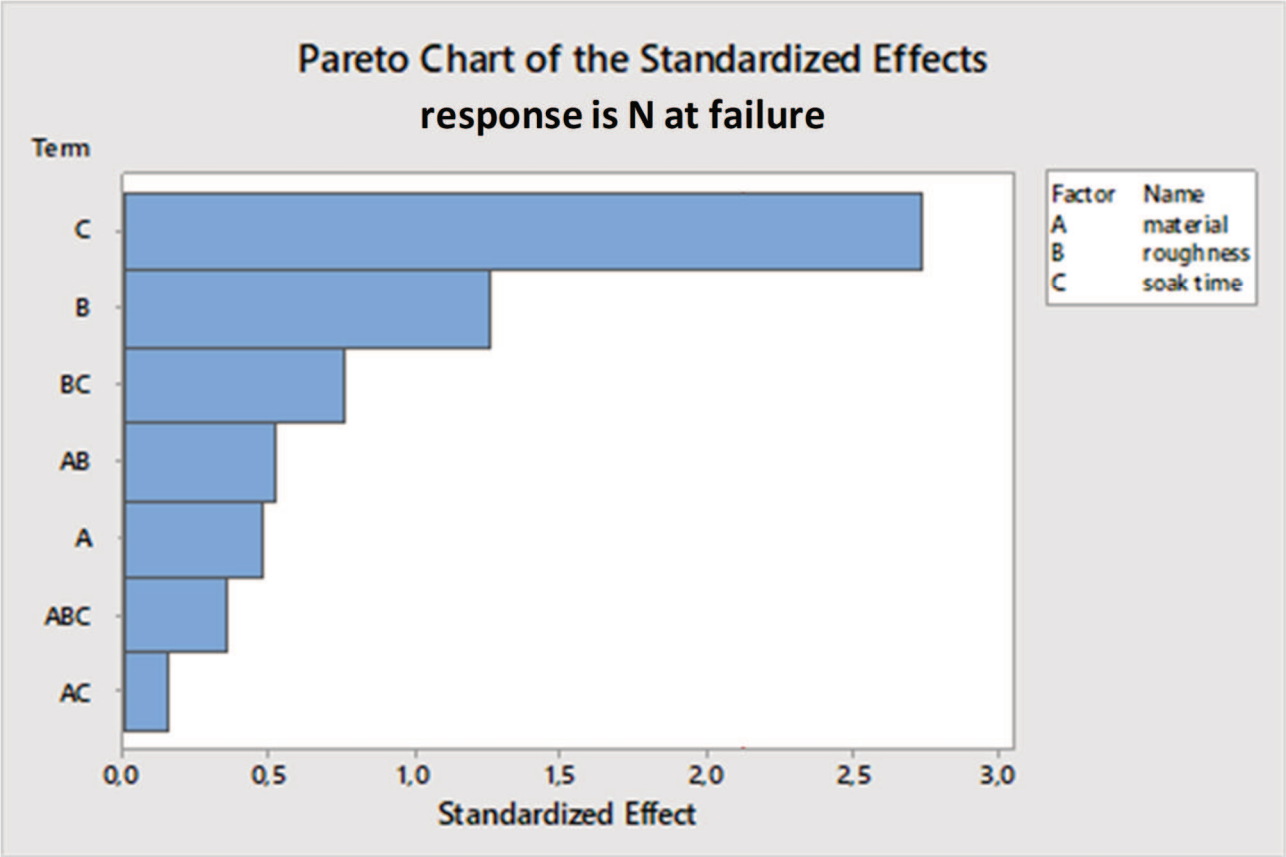

Figure 17. Pareto Chart for Fatigue Life of Al-Al and Al-Mg SLJ tested at F_a = 20% of LTC (F_{mean} = 50% of LTC for respective material pair).

3.3 Failure Mode Analysis

Fracture surfaces of representative test joints were inspected after static and fatigue testing. Visual inspection showed that the prevailing failure mode was interfacial failure. In the case of dissimilar Al-Mg joints, the adhesive always remained attached to the aluminium adherend, while the interfacial failure occurred between the magnesium adherend and the polyurethane adhesive. This demonstrated the higher adhesion of the PE399 film adhesive on the aluminium alloy compared to that on the magnesium alloy. It is also expected that debonding occurs first at the interface with the lower stiffness magnesium adherend due to the higher stress concentration at the ends of the bonded area.

As compared to Al-Mg joints, Scanning Electron Microscope inspection (SEM) in section of fatigue fracture surfaces of Al-Al joints (Figures 18 and 19) showed higher percentage of transferred metal to the adhesive surface. That explains the higher level of degradation of the bond between adhesive and similar aluminium adherends; the higher degradation level of similar-material Al-Al joints would reduce the bond strength under cyclic loading, as compared to dissimilar-material Al-Mg joints. This would provide a possible explanation of why the Al-Mg joints exhibited longer fatigue life; however, the difference in fatigue life data may still be within widely recognized large scatter in fatigue life test data from the same level of fatigue load.

A comparison between the aluminium and magnesium surfaces of two different joints, both tested at high cyclic amplitude, as displayed by SEM inspection is shown in Figures 18-19.

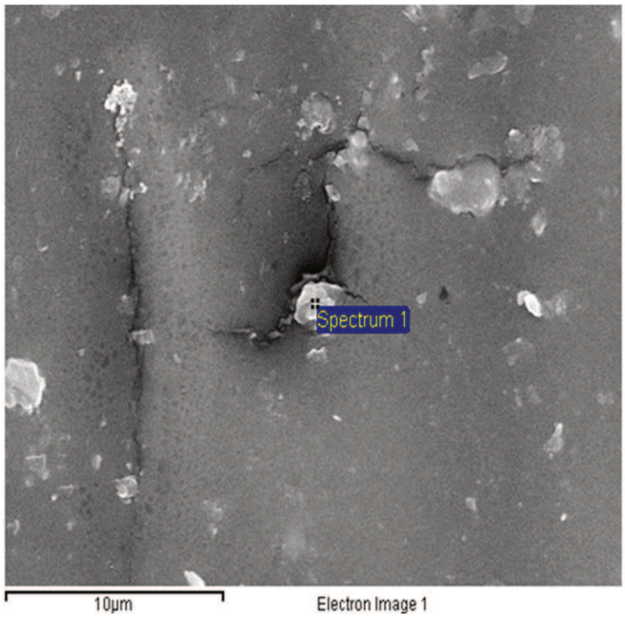

Figure 18. Adhesive Side of Al-Al SLJ, High Amplitude Low Roughness R1.

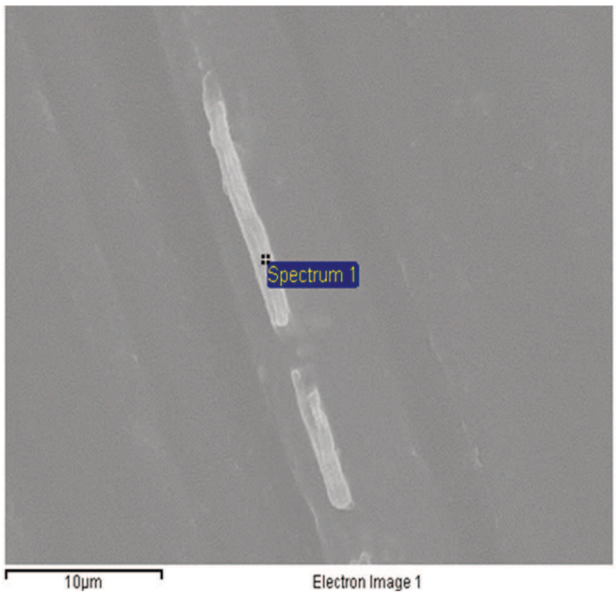

Figure 19. Adhesive Side of Al-Mg SLJ, High Amplitude Low Roughness R1.

The crack in Figure 18 has caused adhesion failure at the aluminium-polyurethane interface; the lighter areas on the adhesive surface correspond to aluminium metal particles. The metal transfer comes from the degradation of the second aluminium adherend.

Figure 19 shows the presence of magnesium (lighter central "strip") on the adhesive surface of the aluminium side of the joint. No cracks are present, and the magnesium particles are not widespread as aluminium particles on the aluminium-aluminium SLJ.

Spectrum analysis of Figure 18 shows the presence of aluminium (33% atomic) together with oxygen (66 % atomic); lighter areas correspond to aluminium oxide particles transferred from the second adherend. Spectrum analysis of Figure 19 detects the presence of magnesium (15% atomic) along with a high atomic percentage of oxygen (83% atomic); this comes from magnesium oxide layer degradation (fretting) at the interface.

5. **Conclusion**

This study provides an insight into the effect of surface roughness and autoclave cure time on static and fatigue performance of film adhesive single lap joints made of lightweight materials, under a tensile-shear loading. A higher roughness of the bond surface resulted in an improvement of the joint static strength, but it reduced joint fatigue life under the selected high mean load that is equal to one half of the joint static strength. Increased static strength is due to the stronger interlocking between the higher surface asperities on the rougher bond surface. Under cyclic loading, however, the larger surface asperities have caused degradation and promoted fatigue crack propagation under cyclic loading. Under the same normalized mean and cyclic load amplitudes (as a percentage of respective static strength), the dissimilar-material joints (Al-Mg) exhibited longer fatigue life than that of the same-material joints (Al-Al). SEM inspection of fracture surfaces showed that the weaker fatigue performance may be mainly attributed to the more relevant surface degradation of Al-Al joints with respect to the Al-Mg joints. This fact was evidenced by the transfer of metal and/or metal oxide from both aluminium substrates to the adhesive layer, as compared to Al-Mg joints. This study showed also that, similar to adhesive joints fabricated with liquid or paste adhesive, the static strength (LTC) of autoclaved film adhesive joints is increased by a longer cure (soak) time, which allows more adhesion strength to develop.

5 Acknowledgement

The authors gratefully acknowledge the guidance of Dr. David Schall with the SEM work, and Ms. Shraddha Jagatap for her help with autoclave use and samples preparation.

References

[1] da Silva LFM, Oechsner A, Adams RD (Eds.). Handbook of Adhesion Technology 2nd ed. Springer, Switzerland, 2018.

[2] Mueller M. Timeline: A Path to Lightweight Materials in Cars and Trucks. Office of Energy Efficiency & Renewable Energy 2016; https://energy.gov/eere/articles/timeline-path-lightweight-materials-cars-and-trucks, last accessed January 2019.

[3] Wegman RF. Surface Preparation Techniques for Adhesive Bonding. Noyes Publ., Westwood, NJ, USA, 1989.

[4] Critchlow G, Brewis D. Review of surface pretreatments for aluminium alloys. Int J Adhes Adhes 1996;16:255-275.

[5] Critchlow G, Brewis D. Influence of surface macroroughness on the durability of epoxide-aluminium joints. Int J Adhes Adhes 1995;15:173-176.

[6] Kim YLY, Yun I-H, Lee J-J, Jung H-T. Evaluation of mechanical interlock effect on adhesion strength of polymer-metal interfaces using micro-patterned surface topography. Int J Adhes Adhes 2010;30:408-417.

[7] Goglio L, Rezaei M. Effect of Different Substrate Pre-Treatments on the Resistance of Aluminum Joints to Moist Environments. J Adhesion 2013;89:769-784.

[8] Crocombe AD, Richardson G. Assessing stress state and mean load effects on the fatigue response of adhesively bonded joints. Int J Adhes Adhes 1999;19:19-27.

[9] Rushforth MW, Bowena P, McAlpine E, Zhou X, Thompson GE. The effect of surface pretreatment and moisture on the fatigue performance of adhesively-bonded aluminium. J Mater Process Tech 2004;153-154:359-365.

[10] Abel M-L, Adams ANN, Kinloch AJ, Shaw SJ, Watts JF. The effects of surface pretreatment on the cyclic-fatigue characteristics of bonded aluminium-alloy joints. Int J Adhes Adhes 2006;26:50-61.

[11] Underhill PR, DuQuesnay DL. The dependence of the fatigue life of adhesive joints on surface preparation. Int J Adhes Adhes 2006;26:62-66.

[12] Nolting AE, Underhill PR, DuQuesnay DL. Variable amplitude fatigue of bonded aluminum joints. Int J Fatigue 2008;30:178-187.

[13] Shenoy V, Ashcroft IA, Critchlow GW, Crocombe AD, Abdel Wahab MM. Strength wearout of adhesively bonded joints under constant amplitude fatigue. Int J Fatigue 2009;31:820-830.

[14] Pirondi A, Moroni F. An investigation of fatigue failure prediction of adhesively bonded metal/metal joints. Int J Adhes Adhes 2009;29:796-805.

[15] Jen Y-M, Ko C-W. Evaluation of fatigue life of adhesively bonded aluminum single-lap joints using interfacial parameters. Int J Fatigue 2010;32:330-340.

[16] Hurme S, Marquis G. Shear fatigue of the bonded and frictional interface under constant normal pre-stress. Int J Fatigue 2015;70:1-12.

[17] Aluminium alloy 6061-T6511 datasheet, http://aluminum.adimetal.com/Asset/adi-6061-t6511-square-bar.pdf, last accessed February 2019.

[18] Magnesium alloy AZ31B-H24 datasheet, AZO materials 2013, https://www.azom.com/article.aspx?ArticleID=8621, last accessed January 2019.

[19] KRYSTALFLEX® PE399 technical datasheet, Huntsman, 2010.

[20] Minitab Statistical Software, DOE Analysis, Effect Plot Analysis.